



**HAL**  
open science

## Degradation of historical paper induced by synchrotron X-ray technical examination

Alice Gimat, Sebastian Schöder, Mathieu Thoury, Anne Laurence Dupont

► **To cite this version:**

Alice Gimat, Sebastian Schöder, Mathieu Thoury, Anne Laurence Dupont. Degradation of historical paper induced by synchrotron X-ray technical examination. *Cellulose*, 2022, 29 (8), pp.4347-4364. 10.1007/s10570-022-04552-3 . hal-03772595

**HAL Id: hal-03772595**

**<https://hal.science/hal-03772595>**

Submitted on 4 Oct 2022

**HAL** is a multi-disciplinary open access archive for the deposit and dissemination of scientific research documents, whether they are published or not. The documents may come from teaching and research institutions in France or abroad, or from public or private research centers.

L'archive ouverte pluridisciplinaire **HAL**, est destinée au dépôt et à la diffusion de documents scientifiques de niveau recherche, publiés ou non, émanant des établissements d'enseignement et de recherche français ou étrangers, des laboratoires publics ou privés.

Copyright

# Degradation of historical paper induced by synchrotron X-ray technical examination

Alice Gimat<sup>1\*</sup>, Sebastian Schöder<sup>2</sup>, Mathieu Thoury<sup>3</sup>, Anne-Laurence Dupont<sup>1\*</sup>

<sup>1</sup> Centre de Recherche sur la Conservation des Collections (CRC, CNRS UAR 3224), Muséum National d'Histoire Naturelle, 36 rue Geoffroy St Hilaire 75005 Paris, France

<sup>2</sup> Synchrotron SOLEIL, 91192 Gif-sur-Yvette, France;

<sup>3</sup> IPANEMA, CNRS, Ministère de la Culture, UVSQ, USR3461, Université Paris Saclay, 91192 Gif-sur-Yvette, France;

\*corresponding authors: [alice.gimat@mnhn.fr](mailto:alice.gimat@mnhn.fr) and [anne-laurence.dupont@mnhn.fr](mailto:anne-laurence.dupont@mnhn.fr)

*Keywords.* calcium carbonate, cellulose degree of polymerization, gelatin, iron gallate ink, yellowing, UV fluorescence.

## Abstract

This research explores how intrinsic factors such as constituents and degradation state can impact the modifications incurred in aged papers during and after X-ray examination. To this end laboratory model papers, artificially aged, and 18<sup>th</sup> and 19<sup>th</sup> century archival documents, with and without additives (gelatin, calcium carbonate) and iron gallate ink, were exposed to Synchrotron X-ray radiation at doses commonly applied (7 Gy to 4 kGy). The threshold dose of 210 Gy previously shown to incur damage in unaged cotton papers falls in this range. Glycosidic scissions, hydroxyl free radicals, UV luminescence and yellowing were measured immediately after the irradiation, and were monitored over a period of three years. Cellulose depolymerization was lower in the aged papers, as well as in the papers containing calcium carbonate and gelatin, than in the unaged fully cellulosic papers. Compared to the papers with no additives, there were more hydroxyl free radicals in the papers with calcium carbonate and slightly less in the gelatin sized papers. UV luminescence and yellowing both appeared post-irradiation, with a delay of several weeks to months. The papers with iron gallate ink showed limited degradation in the low doses range, most probably due to recombination of the free radicals produced. Doses below 4 kGy did not cause yellowing or UV luminescence of the archival papers within the whole monitoring period. The archival papers in good conservation state depolymerized to the same extent as the model papers, while the most degraded archival papers were less impacted than the latter.

## Introduction

Because they are perceived as non-destructive, X-ray analytical techniques are commonly used to examine historic documents and artworks on paper and gain insight into their materials,

32 manufacturing techniques and history (Creagh 2007; Albertin et al. 2015; IAEA 2016; Kozachuk  
33 et al. 2016; Pouyet et al. 2017). Because they are ionizing, X-rays induce changes in organic (as  
34 well as inorganic) materials, yet the potential damage to the artefacts is never considered. This is  
35 largely due to the fact that very little is known about the degradation incurred and the reactions  
36 involved. This lack of knowledge and awareness underlines the need to investigate the issue.

37 Among the few studies that tackle with this problem, some have shown cellulose depolymerization,  
38 oxidation and changes in the optical properties under X-ray exposures (Mantler and Klikovits 2004;  
39 Kozachuk et al. 2016; Gimat et al. 2020) as well as during yet gamma-ray irradiation (shorter  
40 wavelengths than X-rays) used for mold disinfection (Ershov 1998; Bouchard et al. 2006; Henniges  
41 et al. 2013; Bicchieri et al. 2016) . Our recent results have shown that in quasi-pure cellulose paper,  
42 the impact of X-rays was proportional to the dose (Gimat et al. 2020). Due to the large diversity in  
43 the components and in the degradation state of historic cellulosic artefacts, the global impact of X-  
44 ray photons is however difficult to foresee, hence the rationale for the present study.

45 Paper is made of plant fibers, which besides cellulose, most often also contain other biopolymers  
46 such as hemicelluloses and lignin. Additives, fillers and sizing, are usually added to writing and  
47 drawing quality papers to enhance usability parameters: e.g. reduce water permeability, increase  
48 opacity and enhance brightness. In cultural heritage collections, such papers also often bear media  
49 such as inks and pigments. The materials and chemicals used are diverse. In ambient conservation  
50 conditions, a number of these additives can impact the paper degradation rate. For instance gelatin  
51 (Dupont 2003a) and alkaline minerals (Reissland 1999; Sequeira et al. 2006; Ahn et al. 2012; Poggi  
52 et al. 2016) have been shown to decrease the cellulose depolymerization rate, whereas transition  
53 metals in inks and pigments promote degradation by producing acids and free radicals (Selih et al.  
54 2007; Potthast et al. 2008). If and how additives can impact the radiation-induced degradation of  
55 cellulosic paper is still unknown. The presence of absorbing elements, such as iron in the metal-  
56 gallate ink or calcium in the fillers could have a shielding effect and decrease the nominal X-ray  
57 dose, thereby lowering the degradation impact. Such a shielding effect could also be counteracted  
58 by the free radicals formed via the transition metals, which are known cellulose degradation  
59 promoters (Emery and Schroeder 1974; Jeong et al. 2014). It has been shown that iron-containing  
60 pigments undergo a redox reaction under X-ray radiation (Bertrand et al. 2015; Gervais et al. 2015;  
61 Gimat 2016). Moreover, the structural modification of an additive under irradiation can also affect  
62 the paper degradation rate. For instance, X-rays were shown to produce defects inside calcium

63 carbonate (Kabacińska et al. 2017), whereas polypeptide chains (e.g. gelatin) were shown to  
64 undergo hydrolysis (Moini et al. 2014). Bicchieri et al. have examined the combined impact of the  
65 degradation state and certain paper additives on the degradation incurred by ionizing radiation used  
66 for mold disinfection (Bicchieri et al. 2016). The authors used gamma-rays at a dose of 3 kGy.  
67 They tested cellulose paper Whatman n°1, as well as a commercial permanent paper (with CaCO<sub>3</sub>  
68 filler and optical brighteners, and sized with alkyl ketene dimers), which they pre-degraded by an  
69 acid treatment. The acid treated samples showed less radiation induced depolymerization than the  
70 Control samples, indicating that the degradation state played a role. The permanent paper yellowed  
71 more than Whatman n°1, which was attributed to structural modifications of calcium carbonate and  
72 optical brighteners under gamma radiation. To our knowledge, such study has not been conducted  
73 using X-rays, nor at lower doses used during synchrotron X-ray examination of cellulosic cultural  
74 heritage artefacts. This lack of research motivated the present study, which attempts at better  
75 understanding the mitigated impact of X-rays on paper, depending on the fiber deterioration level  
76 and on the presence of components other than the fibers.

77 Handmade linen rag papers from the 18<sup>th</sup> and 19<sup>th</sup> century and industrially-made cotton linters  
78 papers (Whatman n°1) to which various additives were incorporated (gelatin, calcium carbonate  
79 and iron gallate ink) were exposed to synchrotron X-ray radiation. The aim was (i) to study the  
80 impact of the photon energy and (ii) reach high doses, similar to those used during spectroscopic  
81 examinations with instruments in such large-scale facilities. The papers, some of which had been  
82 previously artificially aged, were irradiated at doses in the range 0.007-4 kGy. The samples were  
83 characterized immediately after the exposure using a multiscale analytical procedure developed in  
84 a previous study (Gimat et al. 2020), which encompasses the macroscopic (yellowing and UV  
85 luminescence) and the microscopic scales (glycosidic scissions and formation of hydroxyl  
86 radicals). The changes were monitored over a period of three years.

87

## 88 **Materials and Methods**

### 89 **Paper samples**

#### 90 *Laboratory-prepared samples*

91 Two types of paper were used: Whatman n°1 (W), which is a commercial paper made of cotton  
92 linters (min. 98% alpha cellulose), and a linen rag paper (R) manufactured using traditional stamper  
93 beating at Moulin du Verger papermill (Puymoyen, France). W and R were used either with no  
94 further modification (Control samples), or upon undergoing various artificial aging treatments  
95 (aged samples), in an attempt to approach the molecular degradation state of centuries old cultural  
96 heritage papers. Two artificial aging conditions, one predominantly hygrothermal (*hyg*) and the  
97 other predominantly oxidative (*ox*), were used to depolymerize and increase the carbonyl content  
98 of cellulose. The conditions were adjusted so as to achieve a similar degree of polymerization (*DP*)  
99 and a different degree of oxidation in the *hyg* and *ox* samples.

100 *Hyg* aging of W and R (samples called W\_*hyg* and R\_*hyg*) was performed according to the TAPPI  
101 method (T 573 sp-15 2015). Glass tubes (Wheaton, 35 mm internal diameter (ID) × 147 mm, 144  
102 mL) were filled with 4.0 g of paper (dry weight), i.e. 4.23 g of paper conditioned at 50% relative  
103 humidity (RH) and 23 °C, based on the value of the equilibrium moisture content (EMC = 5.43  
104 %<sub>wt</sub>) determined with the sorption isotherm. The tubes were hermetically closed and heated at 100  
105 °C in an oven (Mettler UN 55 oven) during 10 days to reach a decrease in *DP* of about 50%.  
106 During *hyg* aging, the relative humidity in the tube stabilizes around 50% thanks to the moisture  
107 contained in the paper so that both hydrolysis and oxidation occur. The weight-average degree of  
108 polymerization (*DP<sub>w</sub>*) of cellulose was measured using SEC-MALS-DRI (details in Physico-  
109 chemical characterizations section) and the copper number (*N<sub>Cu</sub>*) was determined using the  
110 standard method (T 430 cm-99 1999). The total carbonyl groups concentration was derived from  
111 *N<sub>Cu</sub>* using the following formula proposed by Röhrling:  $[CO] = \frac{(N_{Cu}-0.07)}{0.06}$  (Röhrling et al. 2002).  
112 *DP<sub>w</sub>* for W\_*hyg* and R\_*hyg* was 1490 ± 2% and 1961 ± 1.6%, respectively. *N<sub>Cu</sub>* of W\_*hyg* was 0.11.  
113 Oxidative degradation (*ox*) was carried out by immersing W in an aqueous solution of sodium  
114 hypochlorite (0.42-0.62% active chlorine) adjusted to pH 7 with HCl 6 N, during 15 min under  
115 gentle stirring. At this pH, NaClO is known to promote enhanced carbonyl groups formation  
116 (aldehyde, ketone, and carboxyl groups) on C2, C3 and C6, short chain organic acids as well as

117 considerable glycosidic scissions (Nevell 1985). The samples (called  $W_{ox}$ ) were abundantly  
118 rinsed with milli-Q water until neutral pH of the water, and were dried between blotters. The  $DP_w$   
119 for  $W_{ox}$  was  $1352 \pm 2\%$  and  $N_{Cu}$  was 0.42.

120 Some of the  $W_{ox}$  samples additionally underwent a reduction treatment with  $Na(BH)_4$  to reduce  
121 the carbonyl groups produced during the aging (aldehyde and keton functions) to alcohol groups,  
122 and achieve a nearly null  $N_{Cu}$ . To this end, a solution made with anhydrous  $Na(BH)_4$  (Sigma)  
123 (2.91g) dissolved in absolute ethanol (154 mL) was prepared, in which 1.54 g of paper was  
124 immersed and left under gentle stirring during 12 hours (Burgess 1988; Carter 1996). After  
125 reduction, the papers were abundantly rinsed with milli-Q water until the water reached neutral pH,  
126 and were dried between blotters. The samples were called  $W_{red}$ .

127 A portion of the W and R Control samples were sized by immersing the paper sheets in a  $20 \text{ g L}^{-1}$   
128 aqueous solution of type B photographic grade gelatin from cattle bone (Gelita type restoration 1,  
129 Kind & Knox) at  $30 \text{ }^\circ\text{C}$  during 10 minutes. The sheets were then dried vertically at ambient  
130 temperature. The sized samples were named  $W_G$  and  $R_G$ .

131 The dry gelatin uptake (UP) of  $W_G$  and  $R_G$ , determined as  $UP =$   
132  $\frac{m_{sized\ paper\ dry} - m_{unsized\ paper\ dry}}{m_{unsized\ paper\ dry}}$ , was  $4.8\% \pm 0.2$ . Dry masses were calculated subtracting the EMC

133 at  $23 \text{ }^\circ\text{C}$  and 50% RH measured according to the standard method (T 502 cm-07 1998). The UP  
134 value falls in the range of gelatin content in historical papers (Barrow 1972; Barrett 1992) and  
135 corresponds to a substantial amount of size in the paper (qualified as with '+' in Table 1).

136 Some of the  $W_G$  and  $R_G$  samples were used to apply the second compound of interest: iron  
137 gallate ink, also referred to as I (samples called  $W_{GI}$  and  $R_{GI}$ ). The ink was prepared by mixing  
138  $FeSO_4 \cdot 7H_2O$  (Sigma Aldrich, 99%) ( $40 \text{ g L}^{-1}$ ), gallic acid monohydrate (Sigma Aldrich, 99%) ( $9$   
139  $\text{ g L}^{-1}$ ) and gum Arabic (Sigma Aldrich, G9752) ( $140 \text{ g L}^{-1}$ ). The mixture was stirred during 3 days  
140 at room temperature. The amount of gum Arabic used was purposely high in order to limit the  
141 penetration of the ink inside the paper. The iron sulfate vs gallic acid ratio was adapted from a  
142 recipe used in previous work (Rouchon et al. 2011). Large inked strokes (1.5 cm wide each) were  
143 applied side by side with a flat-end metal pen ("Plakat", Brause) in order to cover the whole sample  
144 surface. This procedure was not intended to replicate a quill pen stroke, but to provide a large and  
145 homogeneous inked surface ( $2 \times 1 \text{ cm}^2$ ). The ink penetrated 30 to 112 microns into the paper, *i.e.*  
146 one third to one half of the sheet thickness, as observed with the optical microscope (Fig S1 in the

147 Supplementary data file). The iron content determined by XRF using a previously established  
148 calibration curve (unpublished data) was similar in both samples:  $97 (\pm 5) \mu\text{mol g}^{-1}$  in W\_GI and  
149  $110 (\pm 15) \mu\text{mol g}^{-1}$  in R\_GI, values that are comparable to those in historical documents ( $36\text{-}179$   
150  $\mu\text{mol g}^{-1}$ ) (Rouchon et al. 2011).

151 The third compound added to the papers was  $\text{CaCO}_3$  (samples called W\_Ca). W paper was  
152 immersed in a saturated aqueous solution of calcium hydroxide (95%, Sigma Aldrich) (approx.  $1.4$   
153  $\text{gL}^{-1}$ ) during 1 hour and was dried in ambient air. This was repeated four times successively in order  
154 to achieve a high calcium carbonate content. After each bath, the paper sheets were placed between  
155 two blotters, and the excess solution was removed by applying a 10 kg Cobb test metal roller once  
156 back and forth on the blotters. Then the sheets were dried under weight. The reaction of  $\text{CO}_2$  with  
157 the air when the paper is removed from the solution converts  $\text{Ca}(\text{OH})_2$  to  $\text{CaCO}_3$ , so-called alkaline  
158 reserve (AR). The AR determined according to the standard method (T 553 om-00 2000) was  $1.18$   
159  $\pm 0.06 \text{ mol kg}^{-1}$ , otherwise expressed as equivalent  $6.0\% \pm 0.3$  in  $\text{CaCO}_3$ . Additionally, a  
160 commercial permanent paper made of cotton linters, which contained 7.25% precipitated  $\text{CaCO}_3$   
161 (Krypton parchment, Spixel Inc, formerly Domtar), was used (samples named K). Because it was  
162 manually prepared, Ca distribution inside W\_Ca was less homogeneous than in K paper (Fig. S2  
163 in supplementary data file). All the samples were conditioned prior to use at 50% RH,  $23^\circ\text{C}$   
164 according to the standard method (T 402 sp-08 2013).

165

### 166 *Archival papers*

167 Five archival paper documents from the 18<sup>th</sup> and 19<sup>th</sup> century manufactured with linen rags were  
168 chosen. They were named DCN, SE, LN1, LN5, and M. They all contain gelatin size to different  
169 degree, varying from light to strong, and have different *DP* (Table 1 and Fig. S3 in the  
170 Supplementary data file). SE is a page from an 18<sup>th</sup> century printed volume and has a slightly  
171 brownish hue, which appears darker in the center inked area of the page, due to natural aging. DCN  
172 is a printed decree and has a very faint bluish hue. These two papers seem to have the lowest  
173 amount of sizing (Fig. S4 in the Supplementary data file). The three other documents (LN1, LN5  
174 and M) are individual folios of notarial deed documents. M is a blank paper while both LN1 and  
175 LN5 are handwritten with iron gall ink. In SE, DCN, LN1 and LN5, only ink-free areas were used,  
176 in order to better compare with M. Additionally, to investigate the effect of the iron gall ink on

177 ancient archival paper, the laboratory-made iron gallate ink was applied to some of the M samples  
 178 using large strokes as previously described for papers W\_GI and R\_GI, which yielded a  
 179 homogeneous inked area (sample called M\_I).

180  
 181 **Table 1** Samples characteristics: constituents, aging method, thickness ( $x$ ), equilibrium moisture content (EMC) at 23  
 182 °C and 50% RH (T 502 cm-07 1998), weight-average or viscometric-average (denoted \*) degree of polymerization  
 183 ( $DP_0$ ), pH (T 509 om-15 2002), copper number ( $N_{Cu}$ ) (T 430 cm-99 1999), concentration of total carbonyl groups  
 184 ([CO]) (Röhring et al. 2002), ash content (measured at 525 °C) (T 211 om-02 2002), alkaline reserve (AR) expressed  
 185 as %  $CaCO_3$  (T 553 om-00 2000). Standard deviation (STD) is provided when possible. Cot: cotton papers; lin: linen  
 186 rag pulp papers; ox: oxidative degradation; hyg: hygrothermal aging; red: reduction treatment; nat. natural aging; Ca:  
 187 calcium carbonate filler; I: iron gallate ink; G: gelatin sizing (identified with hydroxyproline spot test, with ++: highest  
 188 size content; +: medium size content; ~: lowest size content (levels defined with a water drop absorption test) (Fig S4  
 189 in the Supplementary data file). n.d. stands for not determined.

190

Sample	fiber	Additive	aging	$x$ μm	EMC % wt	$DP_0$	pH	$N_{Cu} / [CO]$ μmol g <sup>-1</sup>	Ash %	AR % <sub>eq</sub>
W	cot	none	none	170	5.43	2948±2%	6.90±0.02	0.05	<0.1	
W_hyg	cot	none	hyg	151	5.46	1490±2%	6.2±0.2	0.11 / 0.67		
W_ox	cot	none	ox	170	n.d.	1352±2%	6.73±0.02	0.42 / 5.83		
W_red	cot	none	ox/red	170	n.d.	1431±1.1%	6.41±0.05	0.02		
W_G	cot	G+	none	170	6.13	3021±1%	5.70			
W_GI	cot	G+, I	none	170	6.90	2225*	4.21			
K	cot	Ca	none	100	5.61	2566±2%	8.89		7.6	7.3
W_Ca	cot	Ca	none	170	5.20	2803±2.2%	8.86		5.4	6.0
R	lin	none	none	160	5.78±0.18	2980	7.90			
R_hyg	lin	none	hyg	141	n.d.	1961±1.6%	6.14			
R_G	lin	G+	none	160	6.57	3326±6.8%	7.68			
R_GI	lin	G+, I	none	150	7.21	2290*	5.15			
SE	lin	G~	nat	115	5.46	1000±9.4%	5.90			
LN5	lin	G++	nat	125	5.36	1039±5.7%	4.92		1.1	
M	lin	G++	nat	125	5.75±0.04	1490±12.8%	5.03		1.5	
M_I	lin	G++, I	nat	125	n.d.	702*	n.d.			
LN1	lin	G+	nat	165	5.12	1608±2.3%	5.28		0.8	
DCN	lin	G~, Ca	nat	90	6.01	2869±6.2%	7.61		2.5	

## 191 Synchrotron X-ray radiation exposures

192 The papers were cut into a few cm<sup>2</sup> samples, inserted in plastic photography slide frames, and  
 193 heated for 2 h at 40 °C (Memmert UN 55 oven) for gentle moisture desorption. They were then



194 placed 48 h in a climatic chamber at 23 °C and 50% RH for equilibrium moisture regain, after  
195 which they were sealed in LDPE plastic bags where silica gel ProSorb (Atlantis) was added so as  
196 to maintain 50% RH ( $\pm 5\%$ ). The EMC (23 °C, 50% RH) of the papers was determined according  
197 to the TAPPI test method (T 502 cm-07 1998) (Table 1). No moisture leakage was recorded upon  
198 monitoring the RH inside the bags for at least 72 h prior to the synchrotron radiation (SR)  
199 experiment with a temperature/humidity logger (Ibutton® Hygrochron, Measurement Systems  
200 Ltd). The bags were themselves sealed with Escal® film also filled with silica gel to stabilize the  
201 RH to 50% for transportation from the laboratory to the synchrotron facility.

202 The irradiation was performed on the beamline PUMA (SOLEIL synchrotron, Saclay). A  
203 monochromatic beam ( $2 \times 1 \text{ cm}^2$ ) from a double crystal monochromator (DCM) with Si(111)  
204 crystals was used at photon energies of 7.22 keV, 12.5 keV or 18 keV. The samples were exposed  
205 perpendicular to the beam, inside the LDPE bags. The irradiation duration varied to reach various  
206 doses in the range 7 Gy to 4 kGy. The dose  $D$  (Gy) is defined as the total energy deposited per  
207 mass unit of material. As it is not possible to directly measure it via dosimetric techniques, which  
208 would be of limited accuracy in a heterogeneous material such as paper, it was calculated as  
209 follows:

$$210 \quad D = \frac{F \cdot E \cdot t}{m} = \frac{I_0 \cdot (1 - e^{-\mu \cdot x}) \cdot E \cdot t}{\rho \cdot \sigma \cdot x}$$

211 with  $F$ , the absorbed photon flux ( $\text{ph s}^{-1}$ );  $E$ , the energy of X-ray photons (J);  $t$ , the exposure time  
212 (s);  $I_0$ , the incident flux ( $\text{ph s}^{-1}$ );  $m$ , the mass of paper (kg);  $x$ , the thickness of paper (cm);  $\rho$  its  
213 density ( $\text{g cm}^{-3}$ );  $\sigma$ , the beam imprint;  $\mu$  the linear attenuation coefficient ( $\text{cm}^{-1}$ ), which was  
214 determined by measuring the incident and transmitted flux impinging stacked sheets as previously  
215 described (Gimat et al. 2020). The dose rate was obtained by the ratio  $D$  over the exposure time.  
216 For Whatman paper n°1, the dose rate was  $0.71 \text{ Gy s}^{-1}$  at 7.22 keV and 18 keV and  $1.35 \text{ Gy. s}^{-1}$   
217 at 12.5 keV.

## 219 **Physico-chemical characterizations**

220 After the irradiation, the samples were kept in the dark at 50% RH and 23 °C until analysis. The  
221 analyses were usually performed within 6 days, the latter being the shortest possible duration

222 between the irradiation and the analysis. This allowed for immediate damage assessment. Post-  
223 irradiation monitoring was carried out by regularly re-examining the samples.

#### 224 *Molar masses*

225 The molar mass distribution and the number- and weight-average molar masses of cellulose  $M_n$   
226 and  $M_w$  were determined using Size-Exclusion Chromatography (SEC), except for the inked  
227 samples which were analyzed using viscometry. For SEC, paper samples (3-5 mg) were prepared  
228 and analyzed as described previously (Dupont 2003b). The precision on  $M_w$  was between 0.2 and  
229 4.0 RSD%, depending on the samples.

230  $S$ , the glycosidic scissions concentration, was calculated using  $DP_n$ , with  $DP_n = \frac{M_n}{M_{AGU}} = \frac{N_{AGU}}{N_{molecule_t}}$ ,  
231 where  $N_{AGU}$  is the total number of anhydroglucose units, i.e monomers ( $M_{AGU} = 162 \text{ g mol}^{-1}$ ) and  
232  $N_{molecule_t}$  is the total number of cellulose molecules at any time  $t$  ( $\mu\text{moles}$ ). As each glycosidic bond  
233 scission increases by one the number of cellulose chains, the increase in the concentration of new  
234 chains formed is equal to  $S$ . The number of scissions being equal to  $N_{molecule_t} - N_{molecule_{t0}}$  and  $N_{AGU}$   
235 being equal to  $6170 \mu\text{mol g}^{-1}$  of paper, hence  $S = 6170 \left( \frac{1}{DP_{nt}} - \frac{1}{DP_{nt0}} \right) \mu\text{moles g}^{-1}_{\text{paper}}$  (Whitmore  
236 and Bogaard 1994).

237 In order to avoid polluting the SEC columns with iron,  $DP$  of the gelatin-ink coated samples W\_GI  
238 and R\_GI was measured using viscometry in cupriethylene diamine (CED) (T 230 om-19 1999)  
239 with a capillary viscometer Routine 100 (Cannon-Fenske). Irradiation was carried out four days  
240 after the ink application. Due to experimental constraints, the viscometry measurements were  
241 carried out 29 days after the irradiation. Before the viscometry analysis, the paper samples were  
242 chemically reduced with  $\text{NaBH}_4$  (same treatment as described above) in order to avoid solvent  
243 induced depolymerization. They were dried between blotters and conditioned at 50% RH and 23  
244 °C. The viscometric DP ( $DP_v$ ) was calculated from the intrinsic viscosity  $[\eta]$  using the Mark-  
245 Houwink-Sakurada equation, by applying the coefficients proposed by Evans and Wallis (Evans  
246 and Wallis 1987) :  $[\eta] = 0.91 \times DP_v^{0.85}$ .  $DP_v$  is assumed to be very close to  $DP_w$  as  $M_v$  has been  
247 reported to be closer from  $M_w$  than  $M_n$  (Ross-Murphy 1985). This allows to parallel  $DP_v$  with  $DP_w$   
248 with some confidence. The formula proposed by Dupont et al. (Dupont et al. 2018) was used for  
249 the conversion of  $DP_v$  to  $DP_n$ :  $DP_n = 1575 e^{(DP_w/3536)} - 1575$ .

## 250 *Hydroxyl radicals*

251 The paper samples were soaked for 3 minutes in a methanolic solution of terephthalic acid (TPA)  
252 (98%, Sigma Aldrich) (1 mM). They were left to dry at ambient temperature for 24 h and  
253 conditioned at 23 °C at 50% RH. TPA reacts with hydroxyl free radicals (HO•) in the paper and  
254 produces hydroxyterephthalic acid (HTPA), which accumulates in the paper. HTPA was extracted  
255 from the paper (2-3 mg) by soaking during three hours in 300 µl of phosphate buffer (KH<sub>2</sub>PO<sub>4</sub> 50  
256 mM pH 3.2, 70% water:30% methanol), and was quantified by reverse phase liquid  
257 chromatography with UV and fluorescence detection (RP-HPLC/FLD-DAD) according to a  
258 previously established method (Jeong et al. 2014). HTPA (µmol g<sup>-1</sup>) was calculated with respect to  
259 the paper dry weight, subtracting the additives weight, to correlate sample behavior based on their  
260 cellulosic content only. In order to ensure the quality of the results, it was verified that no HTPA  
261 was formed upon irradiating TPA powder.

## 262 *Colorimetric and UV luminescence measurements*

263 The diffuse reflectance and UV luminescence of the paper samples were measured with a non-  
264 invasive UV-Vis-NIR spectroradiometer (Specbos 1211UV, JETI). For UV luminescence, the  
265 excitation was centered at 365 nm (with full width half-maximum FWHM = 20 nm). Measurements  
266 were normalized to a blue luminescent certified reflectance standard (USFS-461 Spectralon) to  
267 correct for light intensity change with time. The maximum intensity of each UV luminescence  
268 spectrum was used to monitor the global intensity change. To calculate the change the following  
269 formula was used:

$$270 \quad \Delta I(\lambda_{\max}) = I(\lambda_{\max})[irr] - I(\lambda_{\max})[Ctrl]$$

271 with  $I(\lambda_{\max})[irr]$  and  $I(\lambda_{\max})[Ctrl]$  the intensities of luminescence at the wavelength maxima  
272 measured inside (irr) and outside (Ctrl) of the irradiated area, respectively.

273 A spectrophotometer (Konica Minolta, CM-26d) was used to measure the chromaticity  
274 coordinates L\*, a\* and b\* in the CIELAB 1976 system. The variation of the color coordinate b\*,  
275 which spans on the blue-yellow scale, was used to quantify the yellowing expressed as  $\Delta b^* = b^* -$   
276  $b_0^*$  (positive value).

277

## 278 Results and discussion

### 279 Calculation of the SR X-ray dose

280 The extent of radiation damage usually depends on the X-ray dose absorbed by a sample. Different  
281 papers are expected to absorb X-ray differently, especially when heavy elements are present as the  
282 latter increase the absorption. Defining the X-ray dose is thus essential in order to compare changes  
283 in paper samples after irradiation on a common basis. In order to do so, it is necessary to define the  
284 linear attenuation coefficient ( $\mu$ ) of each sample for each experimental setup and condition. The  
285 value of  $\mu$  was measured with the incident and transmitted flux impinging stacked sheets as  
286 previously described (Gimat et al. 2020). This value depends on the sample characteristics and on  
287 the X-ray energy. Indeed,  $\mu$  decreases with increasing energy, mainly due to the decrease of  
288 photoelectric effect. The values of  $\mu$  measured for W were:  $4.29 \pm 0.07 \text{ cm}^{-1}$  at 7.22 keV,  $1.02 \pm$   
289  $0.06 \text{ cm}^{-1}$  at 12.5 keV and  $0.31 \pm 0.031 \text{ cm}^{-1}$  at 18 keV. The values of  $\mu$  for all the papers at 7.22  
290 keV are given in Table 2. These values fell in the same range for the archival papers and the model  
291 papers. As expected, the values in the table show a positive variation of  $\mu$  with the paper's density  
292 ( $\rho$ ). Indeed, in denser papers the beam path crosses more absorbing atoms. A plot of  $\mu$  vs  $\rho$  (Fig.  
293 S7 in Supplementary data file) shows that for all the papers the two values are actually strongly  
294 positively correlated, and that  $\rho$  explains most of the variation in  $\mu$ , sometimes all the variation,  
295 depending on the samples. For instance, for gelatin sized papers (W\_G, R\_G), degraded model  
296 (W\_hyg, W\_ox and R\_hyg) and archival papers, a higher  $\mu$  compared to the Control samples was  
297 ascribable exclusively to a higher paper density. However, for some samples, there was an  
298 additional input to  $\mu$ . This is the case for samples W\_Ca and K, and was attributed to the presence  
299 of Ca. Ca is a heavy element and has a higher photon absorption than the atoms in cellulose. It was  
300 thus expected that Fe in the inked samples would have the same impact on  $\mu$  when compared to the  
301 counterpart samples with no ink. This was indeed the case for R\_GI and M\_I, but not for W\_GI  
302 (Fig. S7 in Supplementary data file).

303

304 **Table 2** Linear attenuation coefficient  $\mu$  ( $\text{cm}^{-1}$ ) with standard deviation and density ( $\rho$ ) of the studied papers at 7.22  
305 keV, 50% RH.

306

	Cotton papers		Linen rag papers		Archival papers (gelatin sized)			
	$\mu$ cm <sup>-1</sup>	$\rho$ g cm <sup>-3</sup>	$\mu$ cm <sup>-1</sup>	$\rho$ g cm <sup>-3</sup>	$\mu$ cm <sup>-1</sup>	$\rho$ g cm <sup>-3</sup>		
W	4.29 ± 0.07	0.51	R	5.01 ± 0.25	0.54	LN5	5.60 ± 0.23	0.62
W_G	4.76 ± 0.02	0.54	R_G	4.77 ± 0.07	0.53	M	5.69 ± 0.03	0.47
W_GI	7.03 ± 0.04	0.62	R_GI	7.99 ± 0.08	0.55	M_I	10.05 ± 0.03	0.72
W_Ca	6.89 ± 0.12	0.54				SE	6.66 ± 0.04	0.64
K	9.56 ± 0.20	0.68				LN1	7.21 ± 0.10	0.68
W_hyg	5.32 ± 0.07	0.55	R_hyg	5.69 ± 0.28	0.60	DCN	8.18 ± 0.60	0.72
W_ox	5.66 ± 0.14	0.53						
W_red	5.28 ± 0.04	0.53						

307

### 308 *DP and hydroxyl radicals*

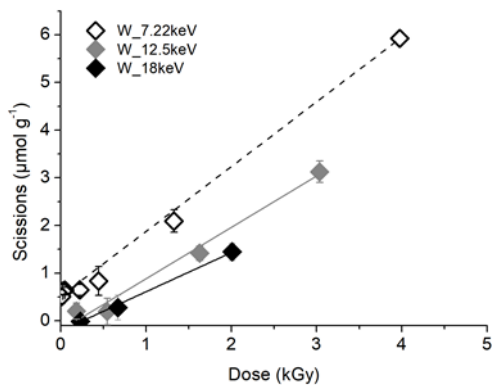
#### 309 Impact of the X-ray dose and photon energy

310 All the X-ray radiation exposures were carried out on the PUMA beamline at synchrotron SOLEIL.  
311 Nevertheless, a first experiment, was carried out with a laboratory Micro X-ray Fluorescence  
312 Spectrometer (methodology in the Supplementary data file), to allow assessing the impact of low  
313 doses in the range of those usually delivered by these laboratory instruments. All the unaged W  
314 samples, irradiated to a dose up to 22 Gy, had a similar *DP* to the Control sample (Fig. S8 in the  
315 Supplementary data file), indicating that no macromolecular degradation took place during the  
316 irradiation, whether the dose was delivered at once or in several stages. This is consistent with the  
317 lowest observable adverse effect dose (LOAED) for glycosidic scissions of 0.21 kGy defined in  
318 our previous work (Gimat et al. 2020).

319 Synchrotron X-ray fluorescence experiments usually use energies in the range of 1 to 20 keV  
320 (Glaser and Deckers 2014), sometimes even higher if heavy elements are investigated. To  
321 investigate if the degradation was energy dependent, W samples were exposed to three photon  
322 energies: 7.22, 12.5 and 18 keV. Fig. 1 shows the glycosidic scissions concentration (*S*) as a  
323 function of the absorbed dose up to 3.9 kGy, at the three energy levels. *S* increased with the dose  
324 in the range of 0 to 6  $\mu\text{mol g}^{-1}$ . The impact was very small below the LOAED (0.21 kGy) and was  
325 followed by a linear increase from 0.5 kGy upwards. *S* increased steeply, similarly at 12.5 keV and  
326 18 keV. At 7.22 keV, all the values of *S* were shifted up. A similar energy dependence has been  
327 observed for electron beam irradiation (Bouchard et al. 2006) at energies of several MeV. While

328 the photoelectrons created by the X-ray photons in our experiment have much lower energies, it  
329 seems like the inverse relation between kinetic energy and cellulose damage remains true in the  
330 keV regime. We are not sure why this is the case, but it is noteworthy that the inelastic mean free  
331 path (IMFP) varies considerably for electron energies in the range of our experiment compared to  
332 the typical average diameter of cellulose fibers. The IMFP for electrons in graphite changes from  
333 9.2 nm at 7.3 keV to 19.5 nm at 18 keV (Shinotsuka et al. 2015). While the exact path lengths in  
334 cellulose will likely be slightly different, this shows that it is thus much more probable that a  
335 photoelectron produced by 18 keV X-rays escapes the cellulose fibers before causing damage than  
336 it is for one produced by 7.22 keV X-rays. Although a lower dose rate can sometime increase  
337 material damage (Adamo et al. 2001), this was not observed here since glycosidic scissions  
338 concentration was higher at 7.22 keV than at 18 keV at similar dose rate ( $0.7 \text{ Gys}^{-1}$ ), yet it was  
339 intermediate at 12.5 keV at higher dose rate ( $1.35 \text{ Gy} \cdot \text{s}^{-1}$ ) (Fig. 1). Based on these results, all the  
340 following experiments were carried out at 7.22 keV, the most penalizing conditions, to enhance the  
341 chances of observing and characterizing damage.

342



343

344 **Fig. 1** Glycosidic scissions concentration  $S$  as a function of the X-ray dose in Whatman n°1 irradiated at energy of  
345 7.22, 12.5 and 18 keV at 50% RH

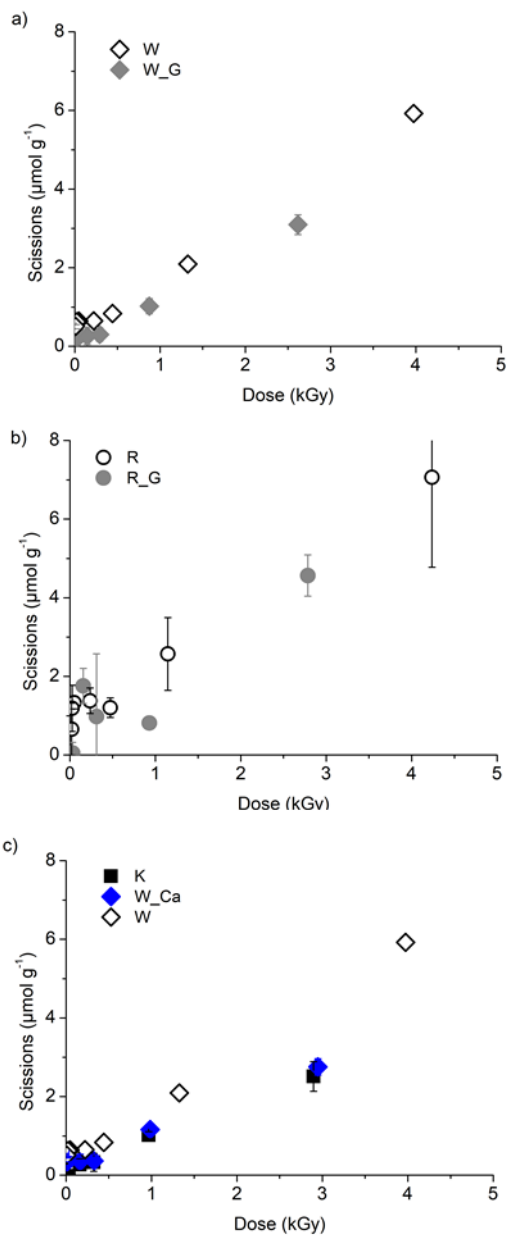
#### 346 Impact of calcium carbonate and gelatin

347 The glycosidic scissions and hydroxyl free radicals concentrations in the unaged papers, in the  
348 papers with calcium carbonate and in the papers with gelatin increased in a quasi linear fashion as  
349 a function of the X-ray dose, up to  $6 \mu\text{mol g}^{-1}$  for W and up to  $8 \mu\text{mol g}^{-1}$  for R (Figs. 2 & 3).  $S$  in  
350 W\_G was slightly lower than in W Control (Fig. 2a). This is consistent with the fact that gelatin

351 size tends to lower the depolymerization rate of cellulose during the degradation induced by aging  
352 (Dupont 2003a). Besides gelatin, this could also be partly due to the difference in moisture in  
353 unsized vs sized paper (EMC at 23°C of 5.43% and 6.13%, respectively), as moisture was shown  
354 to reduce cellulose depolymerization during synchrotron X-ray irradiation (Gimat et al. 2020).  
355 Because of a larger standard deviation on the data points, this was less clearly established for R  
356 and R\_G, where *S* values were quasi similar (Fig. 2b) despite the EMC difference (5.78% vs 6.57%,  
357 respectively) (Table 1).

358 The samples with gelatin (W\_G and R\_G) produced less hydroxyl radicals than the Control  
359 samples (Fig. 3a and 3b). This could be an indication that gelatin was able to scavenge the HO•  
360 produced during the irradiation.

361 In both W\_Ca and K, *S* increased slightly less as a function of the dose than in W Control, which  
362 is especially visible at the high doses, as shown on Fig. 2c. this suggests that calcium carbonate  
363 can buffer the organic acids generated by cellulose degradation caused by the X-ray exposure,  
364 which is the expected role of the alkaline reserve in paper (Whitmore and Bogaard 1994; Ahn et  
365 al. 2013; Rouchon and Belhadj 2016). On the other hand, W\_Ca and K showed a larger HO•  
366 production than the Control samples (Fig. 3c). This, again, could be due to the pH, as an alkaline  
367 medium is known to enhance the lifetime of HO• radicals, and hence the probability that they react  
368 with TPA. These results also confirmed previous observations that the HO• concentration did not  
369 always correlate directly with the glycosidic scissions concentration, and indicate that other species  
370 and mechanisms are involved (Jeong et al. 2014; Gimat et al. 2020).

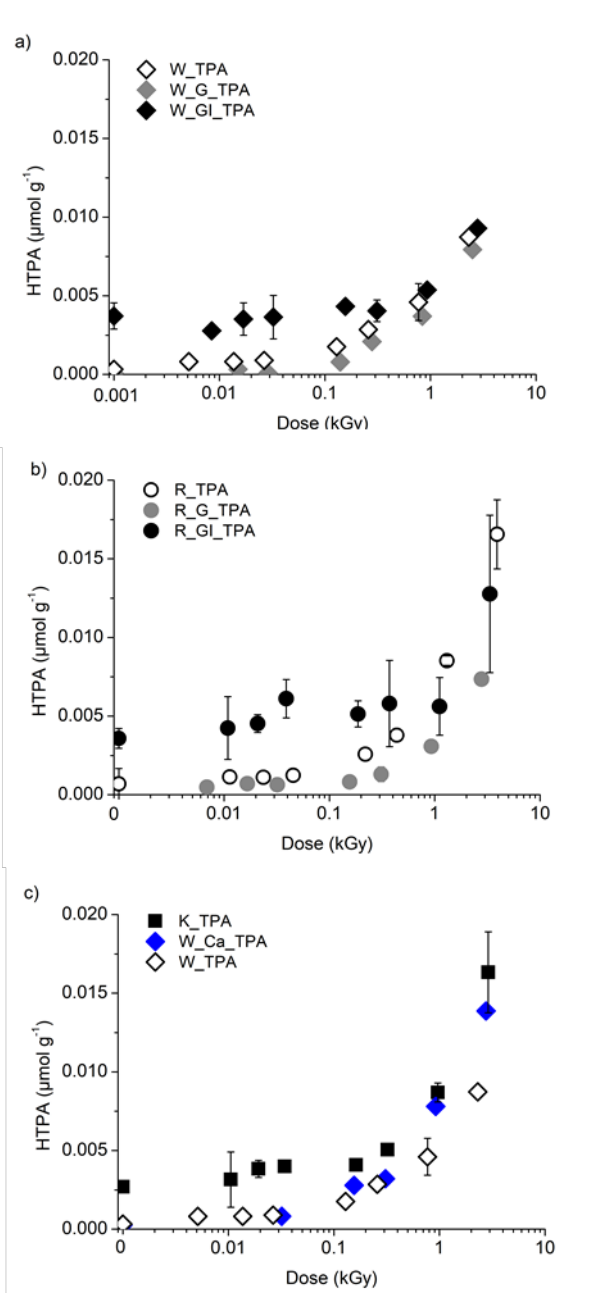


372

373 **Fig. 2** Glycosidic scissions concentration ( $S$ ) in W and R Control papers, papers with gelatin (W\_G and R\_G) (a, b)

374 and with calcium carbonate (W\_Ca and K) (c), as a function of X-ray dose after irradiation at 7.22 keV.





375

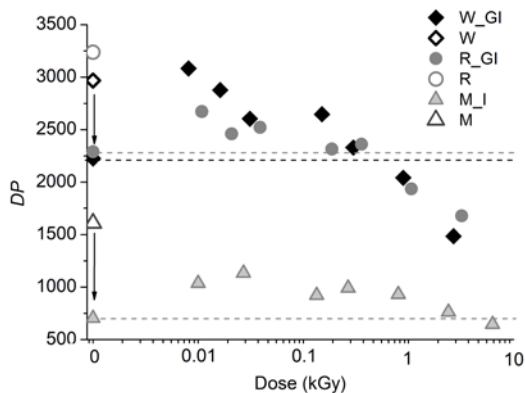
376 **Fig. 3** Impact of gelatin, iron gallate ink (a, b) and calcium carbonate (c) in W and R papers on the HTPA  
 377 concentration as a function of X-ray dose after irradiation at 7.22 keV. The logarithmic scale is used for easier  
 378 visualization.

379

380 Impact of the iron gallate ink

381 For the three samples coated with the iron gallate ink (W\_GI, R\_GI and M\_I), the *DP* of the non-  
 382 irradiated samples was considerably lower than that of the Control samples (W, R and M) is

383 represented by the arrows on Fig. 4. This was attributed to strong and almost instant acid hydrolysis  
384 and oxidation reactions due to the presence of iron gallate ink, which occurs within the period  
385 between sample preparation and analysis (33 days). This has been observed previously (Rouchon  
386 et al. 2011, 2016). Indeed, a *DP* loss of 25% and 30% was measured for W\_GI and R\_GI,  
387 respectively, which is consistent with previous observations (Rouchon et al. 2011) for inked  
388 Whatman n° 1 where a 24% *DP* loss was recorded within a similar timeframe. For M\_I samples,  
389 the *DP* loss was 50%. A striking observation was made in the low doses range: after irradiation (up  
390 to 0.29 kGy for W\_GI, 0.36 kGy for R\_GI and 2.4 kGy M\_I), the *DP* of the iron gallate ink coated  
391 samples was higher than the *DP* of their non-irradiated counterpart (Fig. 4, dashed lines). This is  
392 the reason why *DP* is represented instead of glycosidic scissions as y-axis on Fig. 4. This was  
393 interpreted as having two possible causes. First, it has been shown that iron gallate ink containing  
394 papers produce free radicals, such as HO• and other reactive oxygen species (Gimat et al. 2016,  
395 2017). This enhances the chances for free radicals recombination leading to the auto-oxidation  
396 termination reactions, and in turn would lower the concentration of radicals accumulated in the  
397 paper, thus, possibly preserving cellulose from their attack. Conversely in the Control samples,  
398 unexposed to X-rays, the free radicals would induce a higher level of degradation. Secondly, the  
399 crosslinking induced by the recombination of cellulosic radicals could lead to an increase in *DP*  
400 which would be measurable if the radicals have a relatively high molar mass. This is consistent  
401 with the fact that in the low irradiation doses range, HTPA was produced in higher amount in the  
402 irradiated ink coated samples W\_GI and R\_GI than in the Control counterparts W and R (Fig. 3a,  
403 3b), and in similar amount as in non-irradiated W\_GI and R\_GI. In the higher doses range (from  
404 0.89 kGy for W\_GI, 1.1 kGy for R\_GI, and 6.3 kGy for M\_I), the samples reached a lower *DP*  
405 than the non-irradiated samples, and the HTPA concentration in the samples reached similar levels  
406 with and without ink. This was interpreted as an indication that the enhanced scissions induced by  
407 the irradiation at the high doses likely exceeded the supposed impact of the free radicals  
408 recombination reactions.  
409



410

411 **Fig. 4** Viscometric-average degree of polymerization ( $DP_v$ ) of iron gallate ink coated papers W\_GI (a), R\_GI (b),  
 412 and M\_I (c) as a function of X-ray dose (kGy) after irradiation at 7.22 keV. The dose is represented on a logarithmic  
 413 scale for easier visualization. Control samples without ink or gelatin are represented by the void data points. Arrows  
 414 represent the  $DP$  drop due to the iron gallate ink. At low X-ray doses, irradiated samples have a higher  $DP$  than non-  
 415 irradiated Control sample (above the dotted lines)

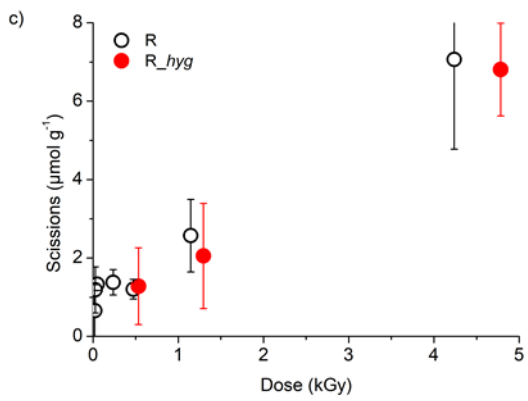
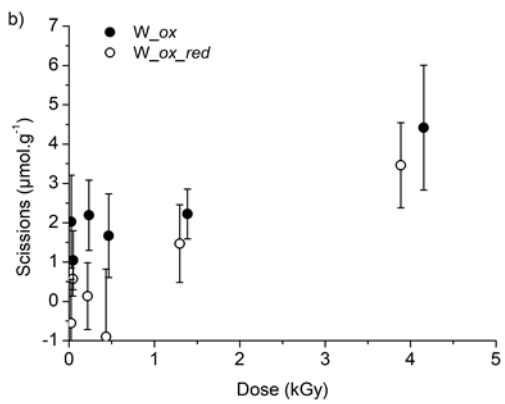
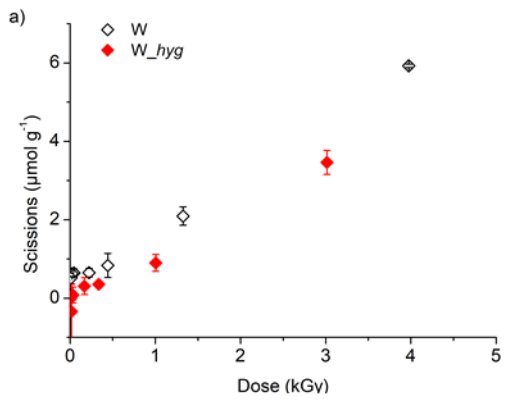
416

417 Impact of the degradation state

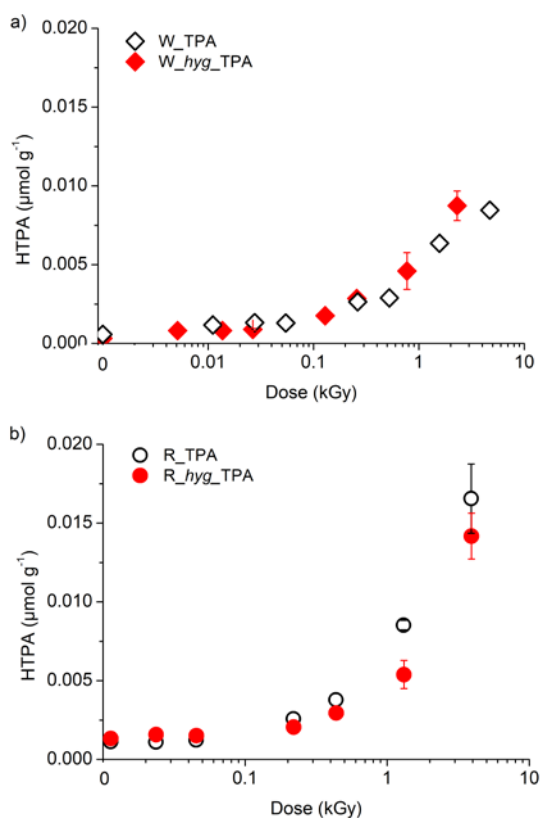
418

419 The artificially degraded papers ( $W_{hyg}$ ,  $W_{ox}$  and  $W_{red}$ ) were irradiated at 7.22 keV to  
 420 various doses to study if and how the degradation state modifies the impact of the X-rays exposure.  
 421 The intent was to possibly extrapolate the results to centuries-old cultural heritage paper. The three  
 422 samples had a similar starting  $DP$  ( $DP_w \approx 1400$ , *i.e.* about 50% lower than W) and a different  
 423 oxidation state:  $N_{Cu} = 0.42$  for  $W_{ox}$  (*i.e.*  $5.83 \mu\text{mol g}^{-1}$  total carbonyl groups, as calculated  
 424 according to (Röhrling et al. 2002),  $N_{Cu} = 0.11$  for  $W_{hyg}$  (*i.e.*  $0.67 \mu\text{mol g}^{-1}$  total carbonyl groups)  
 425 and  $N_{Cu} = 0.02$  for  $W_{red}$  (*i.e.* near-zero carbonyl groups besides the reducing ends) (Table 1).  
 426 Figures 5a and 5b show the glycosidic scissions concentration in these samples as a function of the  
 427 dose. In  $W_{hyg}$ ,  $S$  increased linearly with the dose, yet slightly less than in W Control (Fig. 5a).  
 428 This suggests that lower  $DP$  and/or higher carbonyl groups concentration might lessen somewhat  
 429 the impact of X-rays (Fig S7 in the Supplementary data file). For samples that underwent oxidation  
 430 ( $W_{ox}$  and  $W_{red}$ ),  $S$  was in the same range (up to  $6 \mu\text{mol g}^{-1}$ ) as for W and  $W_{hyg}$  at respective  
 431 doses (Fig. 5b), yet with higher standard deviations. The main contrast between the two samples is  
 432 in the low dose region. In the range –up to 0.5 kGy, while  $W_{red}$  underwent fewer glycosidic  
 433 scissions, in  $W_{ox}$   $S$  was higher than in the other samples, with a sharp increase to 1-2  $\mu\text{mol g}^{-1}$  for  
 434 doses below 1.4 kGy. This tends to indicate that at low doses, a high concentration of carbonyl

435 groups in the paper may enhance the X-ray induced depolymerization. In the higher doses range  
436 ( $\geq 1$  kGy), the depolymerization of all the samples reached the same range, between 4 and 6  $\mu\text{mol}$   
437  $\text{g}^{-1}$ . Fig 6a shows that a similar amount of  $\text{HO}^\bullet$  free radicals was produced in *W\_hyg* and in *W*,  
438 indicating that the free radicals were not fully responsible for the difference in the glycosidic  
439 scissions, and that the  $\text{HO}^\bullet$  were not significantly involved in the production of carbonyl groups.  
440 The results for the linen rag model papers are more difficult to interpret. *S* extended higher (up to  
441  $8 \mu\text{mol g}^{-1}$ ) and increased linearly as a function of the dose, yet, in a similar way for the undegraded  
442 Control sample and for the degraded *R\_hyg*, despite the *DP* of the latter being 34% lower ( $DP_w \approx$   
443 *1961*) (Fig. 5c). Moreover, above 0.1 kGy, slightly less  $\text{HO}^\bullet$  free radicals were detected in *R\_hyg*  
444 than in *R* (Fig. 6b). This, and the large standard deviations on each data point of *R* samples muddles  
445 the interpretations. The extrapolation of the results from a simple machine-made cellulosic paper  
446 to a traditional handmade rag pulp paper is not straightforward. The next level of complexity, which  
447 was to test the response of archival papers, was thus anticipated as very challenging.



448  
 449 **Fig. 5** Glycosidic scissions concentration ( $S$ ) in aged papers  $W$  (a, b) and aged rag papers  $R$  (c) as a function of X-ray  
 450 dose compared to respective Control samples.



451 **Fig. 6** HTPA concentration in Control samples, aged W (a) and aged R (b) as a function of X-ray dose.

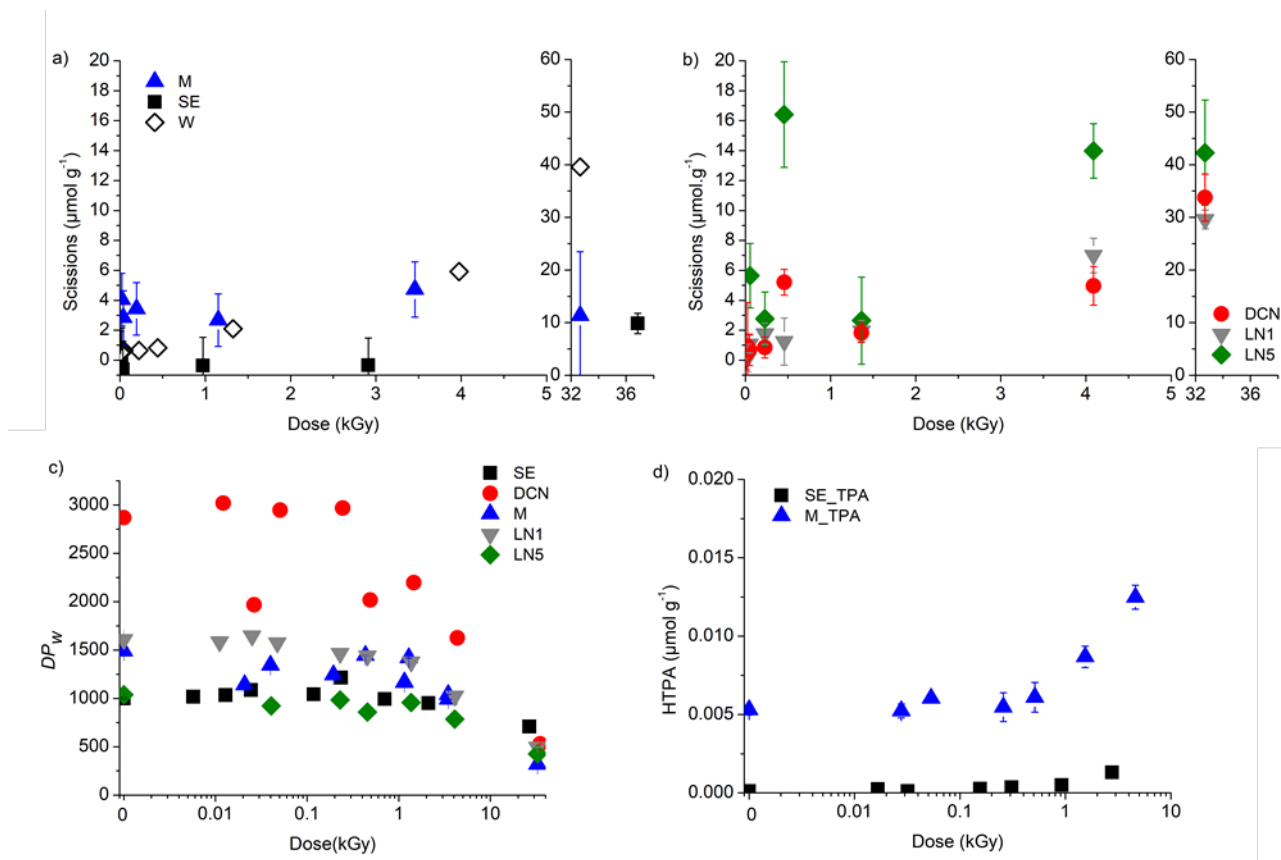
452

453 **Archival paper documents**

454 For the historic samples irradiated to various doses, *S* values were overall in the same range as  
 455 those measured for the model samples. Only LN5 degraded more and showed *S* values at least  
 456 twice as high as for the other archival papers at all the doses tested (Figs. 7a, 7b). However, the  
 457 depolymerization behavior with increasing dose was not progressive as observed for the model  
 458 papers (except for LN1), especially in the low doses. For instance, SE did not undergo scissions  
 459 below 3 kGy, and M had a constant degradation (plateau) response on the whole dose range, with  
 460 *S* around 3.5 μmol g<sup>-1</sup> (Fig. 7a). No correlation could be made with the *DP* (table 1), or the paper  
 461 constituents. All the papers have similar iron and calcium content, except maybe DCN which has  
 462 more calcium due to the calcium carbonate filler and slightly more Fe (Fig. S6 in the Supplementary  
 463 data file). The other possible difference in composition would be the gelatin content, the latter  
 464 being a factor that tends to lower the degradation in the model papers. Unfortunately, the gelatin  
 465 content of the archival papers was unknown and could not be measured. However, an indirect

466 indication of sizing was given by a water drop absorption test, which showed that M and LN5 were  
467 more hydrophobic than DCN (fig. S4 in the Supplementary data file). Even though there can be  
468 other reasons for paper hydrophobicity such as reduced porosity for instance, the former two  
469 showed higher  $S$  than the latter, which would tend to invalidate the aforementioned protective role  
470 of gelatin. The differences in  $S$  could thus arise from local heterogeneity and to samples' structural  
471 parameters such as porosity or constituents' composition. This was not unexpected as in handmade  
472 papers the additives are usually not as homogeneously distributed at the microscopic level as in  
473 industrial papers.

474 Very high doses, between 32 and 38 kGy, were then tested on the archival papers, as well as on W.  
475 The results showed that DCN, LN1 and LN5 were similarly extensively degraded as W, with  $S$   
476 comprised between 30 and 43  $\mu\text{mol g}^{-1}$  (Figs 7a & 7b). M and SE resisted surprisingly well, being  
477 the least degraded samples, with  $S$  close to 10  $\mu\text{mol g}^{-1}$ . Despite the different kinetics, most samples  
478 approached LODP (Levelling Off Degree of Polymerization) with  $DP_w$  W = 345;  $DP_w$  M = 318;  
479  $DP_w$  LN5 = 426;  $DP_w$  LN1 = 495. The least degraded samples were DCN ( $DP_w$  = 530) and SE ( $DP_w$   
480 = 708) (Fig. 7c). The production of HO• free radicals was measured in SE and M. In SE, HO•  
481 concentration was very low, but it was higher in M over the whole dose range reaching a similar  
482 amount as in the model papers containing Ca and Fe (Fig. 7d). This difference was thus attributed  
483 to the slightly higher calcium and iron content in M than in SE (Fig. S6 in the Supplementary data  
484 file).



486

487 **Fig. 7** Glycosidic scissions concentration ( $S$ ) (a, b),  $DP_w$  (c) and HTPA concentration (d) in archival samples as a  
 488 function of X-ray dose. Logarithmic scale (c-d) is used only for a better display of the data.

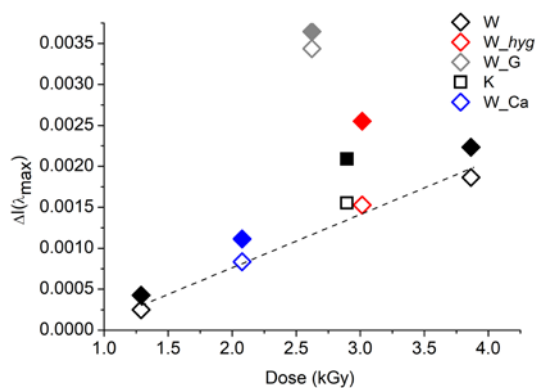
489

#### 490 *UV Luminescence and yellowing*

491 Before the irradiation, all the samples, model and archival, exhibited luminescence under UV when  
 492 excited at 365 nm, which is a common feature of paper (Fig. S9 in the Supplementary data file).  
 493 The model samples W and R exhibited a luminescence maximum  $\lambda_{\text{max}}$  at 432 nm, which is  
 494 consistent with previous data (Gimat et al. 2020). The intensity varied depending on the type of  
 495 additive and on the degradation state, luminophores being produced during the aging. For instance  
 496 gelatin is expected to show a broad luminescence spectrum with  $\lambda_{\text{max}} = 402$  nm (unaged) and 414  
 497 nm (artificially aged at 50% RH and 80° C) (Yova et al. 2001; Duconseille et al. 2016). After X-  
 498 ray exposure, no change in the UV luminescence spectral distribution was observed during the  
 499 three years monitoring period. The intensity at  $\lambda_{\text{max}}$  [ $I(\lambda_{\text{max}})$ ] of each spectrum was followed over



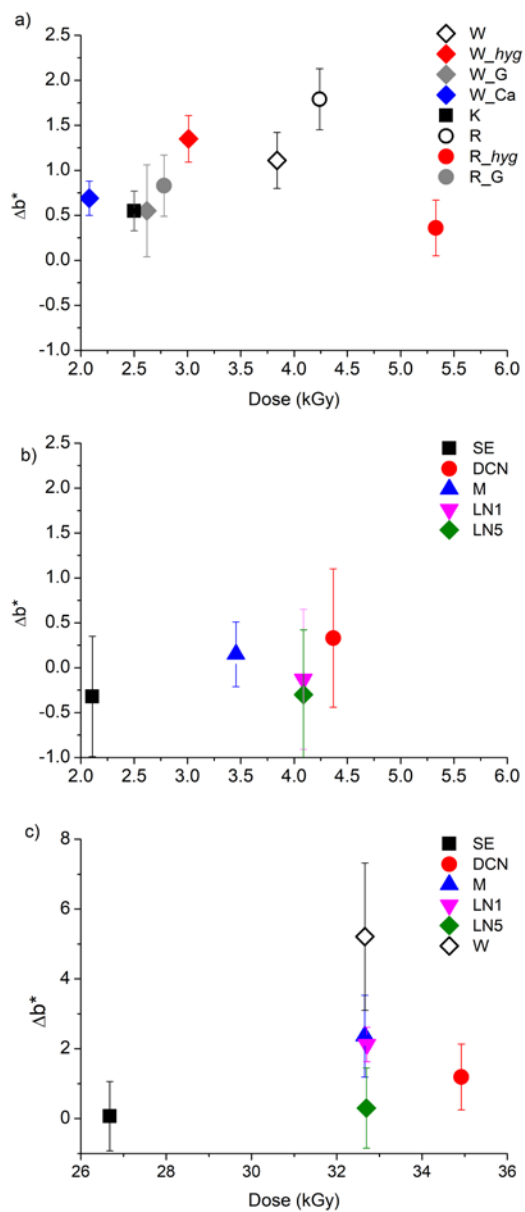
500 time. After eight months, the area of the model papers irradiated at 7.22 keV (dose range from 2.8  
 501 to 4 kGy, depending on the sample) exhibited an increase in the intensity of the UV luminescence  
 502 compared to the respective Control samples ( $\Delta I(\lambda_{\max})$ ), as shown Fig. 8 and Fig. S10  
 503 (Supplementary data file). All Whatman n° 1 model papers (except for the sized samples), showed  
 504 luminescence proportionally to the absorbed dose (Fig 8, white marks, linear trendline). The  
 505 highest increase in luminescence was observed on the sized samples W\_G and R\_G with  
 506  $\Delta I(\lambda_{\max})_{R\_G}$  of 0.0042 and  $\Delta I(\lambda_{\max})_{W\_G}$  of 0.0036 (R\_G data not shown), indicating that a large  
 507 quantity of luminophores was produced post-irradiation. These samples were still the most  
 508 luminescent samples after 11 months. The luminescence of W\_hyg and K grew beyond that of the  
 509 other samples between 8 and 11 months. The change in luminescence between unaged and aged R  
 510 papers (with no additives) was slower than for unaged and aged W, with a smaller  $\Delta I(\lambda_{\max})$  of R  
 511 and R\_hyg (0.0011 and 0.00015, respectively) compared to W and W\_hyg ( $\Delta I(\lambda_{\max})$  (0.0022 and  
 512 0.0025, respectively).



513  
 514 **Fig. 8**  $\Delta I(\lambda_{\max})$  of W, 8 months (empty marks) and 11 months (full marks) after X-ray irradiation.  $\Delta I(\lambda_{\max})$  is the  
 515 subtraction of the luminescence of the non-irradiated area from that of the irradiated area. The trendline represents the  
 516 dose/luminescence response in W Ctrl samples.

517  
 518 Colorimetric measurements were carried out three years after the irradiation, on the irradiated areas  
 519 and the non-irradiated Control samples (Fig. 9). All the model samples showed very small  $\Delta b^*$   
 520 values (Fig. 10a) and a global color change  $\Delta E^*$  between 0.55 (for K) and 1.87 (for R), *i.e.* below  
 521 the usually accepted level for a just noticeable difference. Among the W samples, the artificially  
 522 aged W\_hyg had the highest  $\Delta b^*$  ( $1.35 \pm 0.26$ ). The opposite trend was observed with R samples,  
 523 where R\_hyg had a lower  $\Delta b^*$  than R. This observed behavior difference is all the more valid since

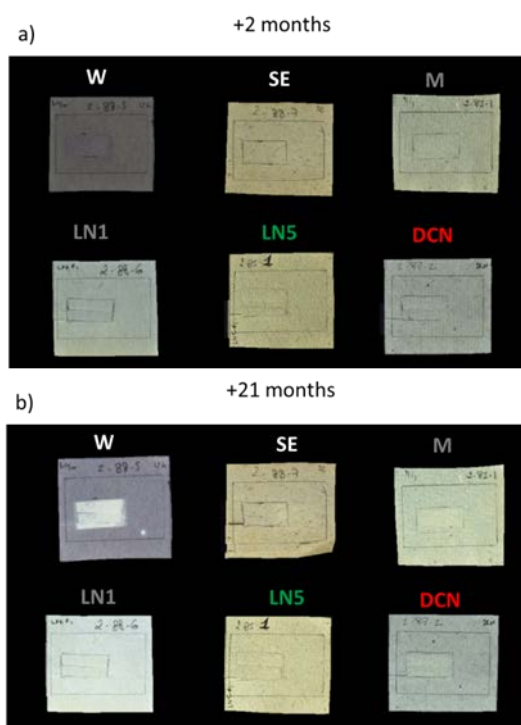
524 the data points for R on Fig 10a correspond to higher doses than for W samples and that R\_hyg is  
525 the most strongly irradiated sample. This may indicate complex radiochemistry mechanisms of  
526 chromophore destruction and chromogens formation. As opposed to the observations after  
527 hygrothermal aging of gelatin sized papers (Dupont 2003a; Missori et al. 2006), the irradiation did  
528 not modify the yellowing in the gelatin sized papers. This may be related to the radical scavenging  
529 properties of gelatin, which could lower the kinetics of cellulose chromophores formation. To sum  
530 up, for the model samples, gelatin was the additive that had the highest impact on luminescence.  
531 This is most probably due to its own intrinsic luminescence properties and maybe also to its  
532 chromogenic degradation products appearing post-irradiation. Yellowing did not appear to be  
533 linked to either the initial degradation state nor to the presence of additives, which indicates  
534 complex mechanisms at play of chromogenic structure formation and destruction.  
535



536  
 537 **Fig. 9** Yellowing increase ( $\Delta b^*$ ) of papers measured three years after X-ray irradiation at 7.22 keV on W and R  
 538 model papers (a) and on the archival papers (b, c).  
 539

540 The initial UV luminescence spectra of the archival papers showed maxima with different  
 541 intensities  $I(\lambda_{\max})$  and positions (between 444 nm and 460 nm), which could be due to differences  
 542 in the quantity and the type of UV-absorbing groups such as carbonyl compounds, respectively.  
 543 This could also be due to a different moisture content, as the latter has been shown to affect the  
 544 luminescence properties of paper (Kocar et al. 2005; Castellán et al. 2007). Before irradiation, no

545 correlation between the state of degradation (*DP*) and the intensity of the luminescence of the  
546 papers could be made. Indeed, LN1 and M, both with similar *DP* around 1500, displayed more  
547 intense luminescence than the other historic samples, either more degraded ( $DP_w$  LN5 =  $1039 \pm$   
548  $5.7\%$ , and  $DP$  SE =  $1000 \pm 9.4\%$ ) or less degraded ( $DP$  DCN =  $2869 \pm 6.2\%$ ). The presence of  
549 gelatin could not be fully responsible of the luminescence intensity either, as the the hydrophobic  
550 properties - used as an indication of the gelatin content - did not correlate with luminescence (M  
551 and LN5 highly hydrophobic, LN1 medium hydrophobic, SE and DCN not hydrophobic).  
552 After irradiation at doses below 4.4 kGy no change was observed on the archival papers. Indeed,  
553 no differences in the UV luminescence (data not shown) nor the yellowing ( $\Delta b^* < 1$ ) were  
554 measured in the irradiated vs the non-irradiated areas (Fig. 9b). At the highest doses tested (26-36  
555 kGy), a slight luminescence appeared on M and DCN twenty-one months after the irradiation (Fig.  
556 10). It thus took almost two years for the luminophores to build up inside the archival papers.  
557 Similarly, as with the model samples, no correlation between the luminescence and the *DP*, or the  
558 glycosidic scissions could be made. A test was made by irradiating M at a very high dose (290  
559 kGy), which induced marginal luminescence, and only after ten months (data not shown).



560  
561 **Fig. 10** Photographs under UV light of W and archival papers exposed to X-ray radiation at doses between 26 and 33  
562 kGy, 1 month (a) and 21 months (b) after the irradiation at 7.22 keV.  
563

564 Within the high dose range (26-36 kGy), no change was observed for SE and LN5, and the other  
565 archival samples (DCN, M, LN1) exhibited a slight yellowing, with  $\Delta b^*$  of 1.2, 2.4, and 2.1,  
566 respectively (Fig. 9c). The strongest yellowing was recorded on W ( $\Delta b^* = 5.2 \pm 2.1$ ).

567

## 568 **Conclusion**

569 Synchrotron X-ray radiation at energies and doses most often applied for analytical purposes to  
570 paper-based cultural heritage has been shown to be detrimental to one-component cellulosic paper  
571 (Whatman n°1). However, field situations are complex as historic papers are multiparametric,  
572 which interferes with a prediction of the effect of X-ray radiation. They usually are degraded to  
573 some extent and they contain other constituents besides biopolymers, such as papermaking  
574 additives, ink and their degradation by-products. The present research investigated how these  
575 parameters, when studied individually in model papers, could influence the X-ray radiation-  
576 induced degradation. The papers were artificially aged and/or supplemented with additives, which  
577 enabled to single out some of the influential parameters. The additives tested were gelatin as sizing  
578 agent, and calcium carbonate as filler. Iron gallate ink was applied on some of the gelatin-sized  
579 papers, modeling writing/drawing medium. Following the same methodological approach as  
580 developed in a previous publication (Gimat et al 2020), the changes were measured immediately  
581 after the irradiation at the microscopic level (macromolecular and molecular degradation) and the  
582 macroscopic changes embodied by the optical properties (UV luminescence and yellowing) were  
583 monitored time-delayed.

584 In the dose range up to 4 kGy, gelatin-sized samples and samples with  $\text{CaCO}_3$  underwent a slightly  
585 reduced irradiation-induced depolymerization. Surprisingly, up to 0.89-1.1 kGy, the iron gallate  
586 ink coated papers had a higher  $DP$  than the Control samples, which was attributed to a decrease in  
587 the impact of the free radical initiated autooxidation reactions through radicals recombination and  
588 crosslinking. Above these doses, a higher rate of scissions induced by the irradiation prevailed. The  
589 production of hydroxyl free radicals was higher in all the samples containing  $\text{CaCO}_3$ , maybe due  
590 to the increased lifetime of  $\text{HO}^\bullet$  at alkaline pH. The depolymerization behavior of the aged model  
591 samples was different in the industrially-made (Whatman n° 1) and in the handmade papers (linen  
592 rags). Higher degradation state (lower  $DP$ ) tended to stabilize Whatman n°1 paper towards X-ray  
593 radiation, by lowering the macromolecular degradation. Conversely, the aged handmade paper

594 showed a similar amount of glycosidic scissions as the unaged counterpart. Carbonyl groups in the  
595 artificially aged Whatman n°1 papers seemed to increase the glycosidic scissions in the low doses  
596 range, below 0.5 kGy. Confirming previous results (Gimat et al. 2020), the optical changes  
597 appeared with considerable delay, often one year after the irradiation, and could not be directly  
598 correlated to the initial *DP* nor to the glycosidic scissions concentration that grew steadily during  
599 this post-irradiation period (dark storage, room temperature). As expected, the archival papers  
600 made of linen rags had an overall more complex X-ray exposure behavior than the model papers.  
601 Their behavior under X-ray was multifactorial and difficult to predict, whether in terms of *DP*  
602 losses (the largest being for DCN and LN1), luminescence (M and DCN exhibited the higher  
603 luminescence intensity), or yellowing (M and LN1 yellowed the most). These observations led to  
604 the conclusion that in the samples with additives and in the aged/degraded samples, optical changes  
605 (yellowing and luminescence) were mostly uncorrelated. Moreover, as observed with the model  
606 papers, these optical changes were also not directly correlated with the macromolecular state  
607 (depolymerization). These observations underline the complex chemistry triggered by the exposure  
608 to X-rays. At very high doses (26-36 kGy), the archival papers reached the LODP immediately  
609 upon irradiation, similarly as Whatman n° 1. No color change or UV luminescence were observed  
610 within one year after the exposure at those high doses. Twenty-one months after the irradiation,  
611 two archival papers showed a slight UV luminescence. These contrasted results indicate that  
612 laboratory samples have their limitations to model archival/historic papers and that the  
613 radiochemistry at play is complex. However, the observation that, overall, the historic papers  
614 resisted better the X-ray exposures than modern papers is an important step forward that enables  
615 to consider analyzing historic papers with better confidence. This work focused on the paper  
616 material in chemical terms. Considering paper microstructure properties in the future may shed  
617 more light on the limitations encountered.

618 The results of this work underline the significance of studying the damage to artworks induced by  
619 X-ray technical examination. A significant outcome was to show the importance of carefully  
620 choosing the analytical conditions that limit the exposure, thus the dose, when analyzing genuine  
621 artefacts using X-rays. This can be achieved either by applying higher energy, or using low  
622 exposure times, and always maintaining some humidity in the paper, as demonstrated in our  
623 previous work. The mid-range relative humidity value recommended for paper-based cultural  
624 heritage storage is thus a good compromise. Documenting the exact location of the X-ray photons

625 impact and implementing a long-term monitoring of the eventual changes through regular  
626 photographic follow-up under both UV and visible lights are advisable.  
627

## 628 **Acknowledgements**

629 We are grateful to synchrotron Soleil for the access to the PUMA beamline within the proposal  
630 20181723 and to Tülin Okbinoglu for technical help on the beamline. We thank Samia Rebaa and  
631 Naomi Nganzami Ebale, undergraduate chemistry students (Sorbonne Université), for help with  
632 photography and spectroscopy. We also thank Sabrina Paris Lacombe and Oulfa Belhadj for  
633 technical help with Size Exclusion Chromatography and Scanning Electron Microscopy,  
634 respectively.  
635

## 636 **Funding**

637 This research was supported by Paris Seine Graduate School of Humanities, Creation, Heritage,  
638 Investissements d’Avenir ANR-17-EURE-0021-Foundation for Cultural Heritage Science.

## 639 **Authors contributions**

640 Methodology: AG, ALD, MT, SC; PUMA Irradiation Experiment: AG, SC; physico-chemical  
641 characterizations: AG, Writing-original draft preparation: AG, ALD; Writing-review and editing:  
642 AG, ALD, MT, SC; Supervision: ALD, MT, SC.

## 643 **Conflict of Interest**

644 The authors declare that they have no conflict of interest.

## 645 **References**

- 646 Adamo M, Brizzi M, Magaudda G, et al (2001) Gamma radiation treatment of paper in different  
647 environmental conditions: chemical, physical and microbiological analysis. *Restaurator*  
648 22:107–131
- 649 Ahn K, Banik G, Potthast A (2012) Sustainability of Mass-Deacidification. Part II: Evaluation of  
650 Alkaline Reserve. *Restaurator* 33:48–75. <https://doi.org/10.1515/res-2012-0003>
- 651 Ahn K, Rosenau T, Potthast A (2013) The influence of alkaline reserve on the aging behavior of  
652 book papers. *Cellulose* 20:1989–2001. <https://doi.org/10.1007/s10570-013-9978-3>
- 653 Albertin F, Astolfo A, Stampanoni M, et al (2015) Ancient administrative handwritten  
654 documents: X-ray analysis and imaging. *J Synchrotron Radiat* 22:446–451.  
655 <https://doi.org/10.1107/S1600577515000314>

- 656 Barrett T (1992) Evaluating the effect of gelatin sizing with regard to the permanence of paper.  
657 In: The Institute of Paper Conservation: conference papers Manchester 1992. Institute of  
658 paper conservation, Manchester, pp 228–233
- 659 Barrow WJ (1972) Manuscripts and Documents: Their Deterioration and Restoration, 2nd  
660 edition. University Press of Virginia
- 661 Bertrand L, Schöeder S, Anglos D, et al (2015) Mitigation strategies for radiation damage in the  
662 analysis of ancient materials. *TrAC Trends Anal Chem* 66:128–145.  
663 <https://doi.org/10.1016/j.trac.2014.10.005>
- 664 Bicchieri M, Monti M, Piantanida G, Sodo A (2016) Effects of gamma irradiation on deteriorated  
665 paper. *Radiat Phys Chem* 125:21–26. <https://doi.org/10.1016/j.radphyschem.2016.03.005>
- 666 Bouchard J, Méthot M, Jordan B (2006) The effects of ionizing radiation on the cellulose of  
667 woodfree paper. *Cellulose* 13:601–610. <https://doi.org/10.1007/s10570-005-9033-0>
- 668 Burgess HD (1988) Practical Considerations for Conservation Bleaching. *JIC-CG* 13:11–26
- 669 Carter HA (1996) The Chemistry of Paper Preservation: Part 1. The Aging of Paper and  
670 Conservation Techniques. *J Chem Educ* 73:417–420. <https://doi.org/10.1021/ed073p417>
- 671 Castellan A, Ruggiero R, Frollini E, et al (2007) Studies on fluorescence of cellulose.  
672 *Holzforschung* 61:504–508. <https://doi.org/10.1515/HF.2007.090>
- 673 Creagh D (2007) Chapter 1 Synchrotron Radiation and its Use in Art, Archaeometry, and  
674 Cultural Heritage Studies. In: *Physical Techniques in the Study of Art, Archaeology and*  
675 *Cultural Heritage*. Elsevier, Amsterdam, pp 1–95
- 676 Duconseille A, Andueza D, Picard F, et al (2016) Molecular changes in gelatin aging observed by  
677 NIR and fluorescence spectroscopy. *Food Hydrocoll* 61:496–503.  
678 <https://doi.org/10.1016/j.foodhyd.2016.06.007>
- 679 Dupont A-L (2003a) Gelatine sizing of paper and its impact on the degradation of cellulose  
680 during ageing: a study using size-exclusion chromatography. PhD thesis. Universiteit van  
681 Amsterdam
- 682 Dupont A-L (2003b) Cellulose in lithium chloride/N,N-dimethylacetamide, optimisation of a  
683 dissolution method using paper substrates and stability of the solutions. *Polymer*  
684 44:4117–4126. [https://doi.org/10.1016/S0032-3861\(03\)00398-7](https://doi.org/10.1016/S0032-3861(03)00398-7)
- 685 Dupont A-L, Réau D, Bégin P, et al (2018) Accurate molar masses of cellulose for the  
686 determination of degradation rates in complex paper samples. *Carbohydr Polym* 202:172–  
687 185. <https://doi.org/10.1016/j.carbpol.2018.08.134>
- 688 Emery JA, Schroeder HA (1974) Iron-catalyzed oxidation of wood carbohydrates. *Wood Sci*  
689 *Technol* 8:123–137. <https://doi.org/10.1007/BF00351367>



- 690 Ershov BG (1998) Radiation-chemical degradation of cellulose and other polysaccharides. *Russ*  
691 *Chem Rev* 67:315. <https://doi.org/10.1070/RC1998v067n04ABEH000379>
- 692 Evans R, Wallis AFA (1987) Comparison of cellulose molecular weights determined by high  
693 performance size exclusion chromatography and spectrometry. *Proc Fourth Int Symp*  
694 *Wood Pulping Chem Paris* 1:201–206
- 695 Gervais C, Thoury M, Réguer S, et al (2015) Radiation damages during synchrotron X-ray micro-  
696 analyses of Prussian blue and zinc white historic paintings: detection, mitigation and  
697 integration. *Appl Phys A* 121:949–955. <https://doi.org/10.1007/s00339-015-9462-z>
- 698 Gimat A (2016) Comprehension of cellulose depolymerisation mechanisms induced by iron ions.  
699 PhD thesis. Université Pierre et Marie Curie
- 700 Gimat A, Dupont A-L, Lauron-Pernot H, et al (2017) Behavior of cellobiose in iron-containing  
701 solutions: towards a better understanding of the dominant mechanism of degradation of  
702 cellulosic paper by iron gall inks. *Cellulose* 24:5101–5115.  
703 <https://doi.org/10.1007/s10570-017-1434-3>
- 704 Gimat A, Kasneryk V, Dupont A-L, et al (2016) Investigating the DMPO-formate spin trapping  
705 method for the study of paper iron gall ink corrosion. *New J Chem* 40:9098–9110.  
706 <https://doi.org/10.1039/C6NJ01480A>
- 707 Gimat A, Schöder S, Thoury M, et al (2020) Short- and Long-Term Effects of X-ray Synchrotron  
708 Radiation on Cotton Paper. *Biomacromolecules* 21:2795–2807.  
709 <https://doi.org/10.1021/acs.biomac.0c00512>
- 710 Glaser L, Deckers D (2014) The Basics of Fast-scanning XRF Element Mapping for Iron-gall Ink  
711 Palimpsests. *Manuscr Cult* 7:104–112
- 712 Henniges U, Hasani M, Potthast A, et al (2013) Electron Beam Irradiation of Cellulosic  
713 Materials—Opportunities and Limitations. *Materials* 6:1584–1598.  
714 <https://doi.org/10.3390/ma6051584>
- 715 IAEA (2016) Trends of Synchrotron Radiation Applications in Cultural Heritage, Forensics and  
716 Materials Science. International Atomic Energy Agency, Vienna
- 717 Jeong M-J, Dupont A-L, de la Rie ER (2014) Degradation of cellulose at the wet–dry interface.  
718 II. Study of oxidation reactions and effect of antioxidants. *Carbohydr Polym* 101:671–  
719 683. <https://doi.org/10.1016/j.carbpol.2013.09.080>
- 720 Kabacińska Z, Yate L, Wencka M, et al (2017) Nanoscale Effects of Radiation (UV, X-ray, and  
721  $\gamma$ ) on Calcite Surfaces: Implications for its Mechanical and Physico-Chemical Properties.  
722 *J Phys Chem C* 121:13357–13369. <https://doi.org/10.1021/acs.jpcc.7b03581.s001>
- 723 Kocar D, Strlic M, Kolar J, et al (2005) Chemiluminescence from paper III: the effect of  
724 superoxide anion and water. *Polym Degrad Stab* 88:407–414.  
725 <https://doi.org/10.1016/j.polymdegradstab.2004.12.005>

- 726 Kozachuk M, Suda A, Ellis L, et al (2016) Possible Radiation-Induced Damage to the Molecular  
727 Structure of Wooden Artifacts Due to Micro-Computed Tomography, Handheld X-Ray  
728 Fluorescence, and X-Ray Photoelectron Spectroscopic Techniques. *J Conserv Mus Stud*  
729 14:2–6. <https://doi.org/10.5334/jcms.126>
- 730 Mantler M, Klikovits J (2004) Analysis of art objects and other delicate samples: Is XRF really  
731 nondestructive? *Powder Diffr* 19:16–19. <https://doi.org/10.1154/1.1649962>
- 732 Missori M, Righini M, Dupont A-L (2006) Gelatine sizing and discoloration: A comparative  
733 study of optical spectra obtained from ancient and artificially aged modern papers. *Opt*  
734 *Commun* 263:289–294. <https://doi.org/10.1016/j.optcom.2006.02.004>
- 735 Moini M, Rollman CM, Bertrand L (2014) Assessing the Impact of Synchrotron X-ray Irradiation  
736 on Proteinaceous Specimens at Macro and Molecular Levels. *Anal Chem* 86:9417–9422.  
737 <https://doi.org/10.1021/ac502854d>
- 738 Nevell TP (1985) Degradation of cellulose by acids, alkalis and mechanical means. Chapter 9.  
739 In: Nevell TP, Zeronian SH (eds) *Cellulose chemistry and its applications*. Ellis Horwood,  
740 Chichester, pp 223–242
- 741 Poggi G, Sistach MC, Marin E, et al (2016) Calcium hydroxide nanoparticles in hydroalcoholic  
742 gelatin solutions (GeolNan) for the deacidification and strengthening of papers containing  
743 iron gall ink. *J Cult Herit* 18:250–257. <https://doi.org/10.1016/j.culher.2015.10.005>
- 744 Potthast A, Henniges U, Banik G (2008) Iron gall ink-induced corrosion of cellulose: aging,  
745 degradation and stabilization. Part 1: model paper studies. *Cellulose* 15:849–859.  
746 <https://doi.org/10.1007/s10570-008-9237-1>
- 747 Pouyet E, Devine S, Grafakos T, et al (2017) Revealing the biography of a hidden medieval  
748 manuscript using synchrotron and conventional imaging techniques. *Anal Chim Acta*  
749 982:20–30. <https://doi.org/10.1016/j.aca.2017.06.016>
- 750 Reissland B (1999) Ink Corrosion Aqueous and Non Aqueous Treatment of Paper Objects - State  
751 of the Art. *Restaurator* 20:167–180
- 752 Röhring J, Potthast A, Rosenau T, et al (2002) A Novel Method for the Determination of  
753 Carbonyl Groups in Cellulosics by Fluorescence Labeling. 2. Validation and  
754 Applications. *Biomacromolecules* 3:969–975. <https://doi.org/10.1021/bm020030p>
- 755 Ross-Murphy SB (1985) Properties and uses of cellulose solutions. Chapter 8. In: Nevell TP,  
756 Zeronian S (eds) *Cellulose Chemistry and its Applications*. Ellis Horwood, Chichester, pp  
757 202–222
- 758 Rouchon V, Belhadj O (2016) Calcium Hydrogen Carbonate (Bicarbonate) Deacidification: What  
759 you always wanted to know but never dared asking. *J Pap Conserv* 17:125–127.  
760 <https://doi.org/10.1080/18680860.2016.1287406>

- 761 Rouchon V, Belhadj O, Duranton M, et al (2016) Application of Arrhenius law to DP and zero-  
762 span tensile strength measurements taken on iron gall ink impregnated papers: relevance  
763 of artificial ageing protocols. *Appl Phys A* 122:773. [https://doi.org/10.1007/s00339-016-](https://doi.org/10.1007/s00339-016-0307-1)  
764 0307-1
- 765 Rouchon V, Duranton M, Burgaud C, et al (2011) Room-Temperature Study of Iron Gall Ink  
766 Impregnated Paper Degradation under Various Oxygen and Humidity Conditions: Time-  
767 Dependent Monitoring by Viscosity and X-ray Absorption Near-Edge Spectrometry  
768 Measurements. *Anal Chem* 83:2589–2597. <https://doi.org/10.1021/ac1029242>
- 769 Selih VS, Strlic M, Kolar J, Pihlar B (2007) The role of transition metals in oxidative degradation  
770 of cellulose. *Polym Degrad Stab* 92:1476–1481.  
771 <https://doi.org/10.1016/j.polymdegradstab.2007.05.006>
- 772 Sequeira S, Casanova C, Cabrita EJ (2006) Deacidification of paper using dispersions of  
773 Ca(OH)<sub>2</sub> nanoparticles in isopropanol. Study of efficiency. *J Cult Herit* 7:264–272.  
774 <https://doi.org/10.1016/j.culher.2006.04.004>
- 775 Shinotsuka H, Tanuma S, Powell CJ, Penn DR (2015) Calculations of electron inelastic mean  
776 free paths. X. Data for 41 elemental solids over the 50 eV to 200 keV range with the  
777 relativistic full Penn algorithm. *Surf Interface Anal* 47:1132–1132.  
778 <https://doi.org/10.1002/sia.5861>
- 779 T 211 om-02 (2002) Ash in wood, pulp, paper and paperboard: combustion at 525°C. Technical  
780 Association of the Pulp and Paper Industry
- 781 T 230 om-19 (1999) Viscosity of pulp (capillary viscometer method). Technical Association of  
782 the Pulp and Paper Industry
- 783 T 402 sp-08 (2013) Standard conditioning and testing atmospheres for paper, board, pulp  
784 handsheets, and related products. Technical Association of the Pulp and Paper Industry
- 785 T 430 cm-99 (1999) Copper Number of Pulp, Paper, and Paperboard. Technical Association of  
786 the Pulp and Paper Industry
- 787 T 502 cm-07 (1998) Equilibrium relative humidity of paper and paperboard. Technical  
788 Association of the Pulp and Paper Industry
- 789 T 509 om-15 (2002) Hydrogen ion concentration (pH) of paper extracts (cold extraction method).  
790 Technical Association of the Pulp and Paper Industry
- 791 T 553 om-00 (2000) Alkalinity of paper as calcium carbonate (alkaline reserve of paper).  
792 Technical Association of the Pulp and Paper Industry
- 793 T 573 sp-15 (2015) Accelerated temperature aging of printing and writing paper by dry oven  
794 exposure apparatus. Technical Association of the Pulp and Paper Industry

- 795 Whitmore PM, Bogaard J (1994) Determination of the Cellulose Scission Route in the Hydrolytic  
796 and Oxidative Degradation of Paper. *Restaurator* 15:26–45.  
797 <https://doi.org/10.1515/rest.1994.15.1.26>
- 798 Yova D, Hovhannisyan V, Theodossiou T (2001) Photochemical effects and hypericin  
799 photosensitized processes in collagen. *J Biomed Opt* 6:52–7.  
800 <https://doi.org/10.1117/1.1331559>
- 801